7-1-1998

Experimental Observation Of Correlated Magnetic Reconnection And Alfvénic Ion Jets

Thomas W. Kornack , '98

Peter K. Sollins , '98

Michael R. Brown
Swarthmore College, doc@swarthmore.edu

PHYSICAL REVIEW E VOLUME 58, NUMBER 1 JULY 1998

Experimental observation of correlated magnetic reconnection and Alfvénic ion jets

T. W. Kornack, P. K. Sollins, and M. R. Brown
Department of Physics and Astronomy, Swarthmore College, Swarthmore, Pennsylvania 19081-1397
(Received 20 February 1998)

Correlations between magnetic reconnection and energetic ion flow events have been measured with merging force free spheromaks at the Swarthmore Spheromak Experiment. The reconnection layer is measured with a linear probe array and ion flow is directly measured with a retarding grid energy analyzer. Flow has been measured both in the plane of the reconnection layer and out of the plane. The most energetic events occur in the reconnection plane immediately after formation as the spheromaks dynamically merge. The outflow velocity is nearly Alfvénic. As the spheromaks form equilibria and decay, the flow is substantially reduced. [S1063-651X(98)51107-5]

PACS number(s): 52.30.−q, 52.55.Hc, 96.60.Rd

There is growing evidence that magnetic reconnection plays a crucial role in particle acceleration in astrophysical plasmas. Recently, the Yohkoh satellite has produced dramatic images of solar flares correlating x-ray, magnetic, and particle data for the first time. Observations made with the Yohkoh hard-x-ray and soft-x-ray telescopes have identified the reconnection region at the top of the flare as the site of particle acceleration [1]. The so-called Masuda flare has subsequently been studied in great detail. Aschwanden *et al.* [2] measured bursts of x rays with periods on the order of seconds coming from the loop top and footpoints. Timing delays between x rays of different energies reveal several acceleration and escape mechanisms for downward flowing particles that are energized by reconnection [2,3]. Shibata *et al.* [4] detected jets of upward flowing plasma above the Masuda flare close to the Alfvén speed v_{Alf}, providing further evidence of reconnection and conversion of magnetic energy to kinetic energy in flares. Doppler-shift measurements on the Solar and Heliospheric Observatory (SOHO) ultraviolet spectrometer show evidence of bidirectional Alfvénic jets in the reconnection plane [5]. Earthward flowing plasma streams with flow velocities up to 1000 km/s (close to the local Alfvén speed) have been observed after reconnection events in the earth's magnetotail [6].

Recent laboratory experiments by Yamada, Ono, and coworkers have pointed out the importance of three-dimensional effects on the reconnection rate [7–9]. They have also observed ion heating and acceleration by Doppler broadening and shifts of line emission [10], and have identified Y- and O-shaped structures in the reconnection layer [11]. Recent results indicate that classical resistivity is insufficient to explain their observed reconnection rates [12]. Earlier experiments by Gekelman *et al.* also observed ion flow but in an experiment with unmagnetized ions [13]. To our knowledge, no experiment reports flow measurements both in and out of the reconnection plane.

In this Rapid Communication, we present correlated direct measurements of magnetic reconnection and energetic particle events from the merger of two force-free spheromak plasmas at the Swarthmore Spheromak Experiment (SSX) [14]. Magnetic data are recorded along a chord passing perpendicularly through the plane of intersection of the spheromaks. We observe a rapid formation of a reconnection layer (within a few Alfvén transit times of spheromak formation) followed by the appearance of Alfvénic (suprathermal) ion flow at an electrostatic energy analyzer. We have made ion flow measurements both in and out of the reconnection plane and the flow appears to be predominantly in the plane containing the reconnecting field. The thickness of the reconnection layer is consistent with the collisionless two fluid prediction of $\delta \approx c/\omega_{pi}$.

Predictions of the structure and thickness of the reconnection layer depend sensitively on the model used. If parcels of magnetofluid of macroscopic scale L and with oppositely directed magnetic flux are merged at a velocity of v_{in}, then a boundary layer of thickness δ is formed where the opposing flux is annihilated. The resistive magnetic induction equation can be written as

$$\frac{\partial B}{\partial t} = \nabla \times (v \times B) + \frac{\eta}{\mu_0} \nabla^2 B.$$

Resistive magnetohydrodynamics (MHD) predicts that in steady state the two terms on the right-hand side balance. Writing $\nabla \sim 1/\delta$ as an inverse scale length across the layer, this condition can be written as

$$R_m = \frac{\mu_0 v_{in} \delta}{\eta} = 1,$$

where R_m is the magnetic Reynolds number (the ratio of convection to diffusion) based on the inflow velocity and the thickness of the layer. The assumptions of incompressibility and energy conservation yield

$$v_{out} = \frac{L}{\delta} v_{in} = v_{Alf}.$$

The scales and velocities are therefore related by

$$\frac{L}{\delta} = \frac{v_{out}}{v_{in}} = \sqrt{S},$$

where S is the Lundquist number based on the macroscopic scale L ($S = R_m$ if v_{Alf} is used for the velocity). Since $S \propto \eta^{-1}$, resistive MHD predicts [15,16] that the thickness of

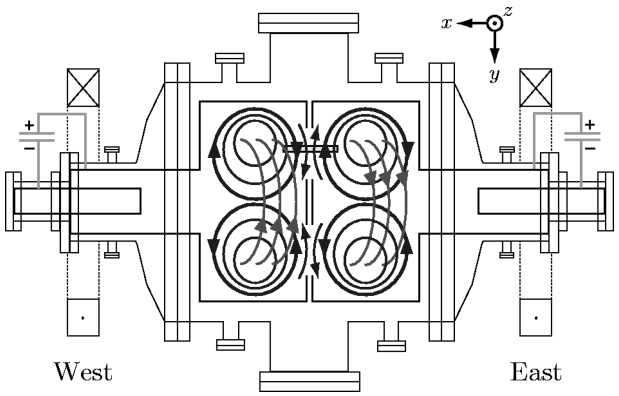

FIG. 1. Schematic of the SSX experiment showing both guns with two large flux conservers to allow reconnection studies. The magnetic-field structure is depicted for a left- (right-) handed spheromak in the east (west) flux conserver. The view is the x-y plane from above.

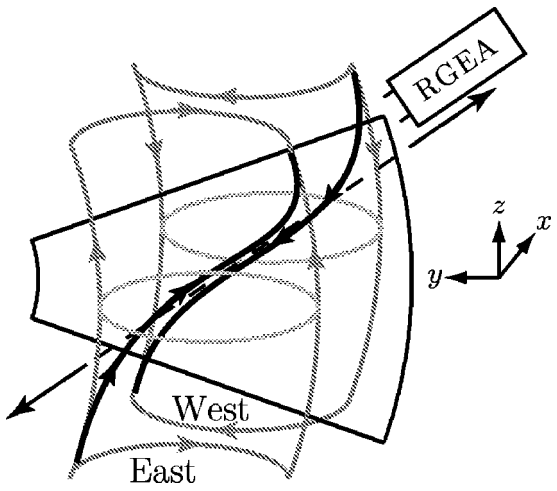

FIG. 2. Local reconnection geometry. The east (west) spheromak is depicted with left- (right-) handed helicity so that the retarding grid energy analyzer is in the reconnection plane.

the layer vanishes like $1/\sqrt{S}$. It has recently been shown [17] that in the collisionless limit of large S (and small η), Hall dynamics and electron inertia govern the scale of reconnection. Electron and ion dynamics decouple on scales that are smaller than the ion inertial length c/ω_{pi} and the thickness of the layer is clamped by ion inertia. Electron dynamics generate an inner scale c/ω_{pe} where the frozen-in flux constraint is broken and reconnection occurs.

Two-dimensional resistive MHD simulations [18] predict the acceleration of a few particles to super-Alfvénic velocities normal to the layer in addition to the Alfvénic flow across the layer. The super-Alfvénic particles are trapped in ''magnetic bubbles'' for a few Alfvén times and are accelerated by the self-consistent electric field at the O point. This energetic tail is predicted to be convected across the layer at v_{Alf}. Collisionless two-and-one-half-dimensional hybrid simulations [19] also predict ion beams (as well as in-plane Alfvénic flow) and significant out-of-plane magnetic fields. As the magnetic flux and electron fluid decouple at the inner scale (c/ω_{pe}) an out-of-plane super-Alfvénic jet of electron fluid is seen. The electron jet drags flux out of the plane to produce out-of-plane magnetic fields.

We are able to generate force-free spheromaks with magnetized plasma guns at SSX [14] and merge them coaxially. Our experimental results corroborate aspects of some of the models and simulations described above. In addition, we are able to reproduce in the laboratory some of the astrophysical processes observed by satellites. Triple probe measurements [20] yield $T_e \approx$ 20 eV and $n_e \approx 10^{14}$ cm^{-3} for SSX plasmas, and our average magnetic field is 500 G. These values give $c/\omega_{pi} \approx$ 2 cm and $S \lesssim 1000$, and predict a resistive reconnection layer thickness $\delta < 1$ cm. If $T_i \simeq T_e$, then $\rho_i \lesssim 1$ cm. The collisional mean free path is $\approx$10 cm and the Alfvén speed is about 10^7 cm/s.

Figure 1 shows the experimental arrangement with the orientation of the magnetic probe and Fig. 2 shows a schematic depicting the energy analyzer with respect to the toroidal and poloidal fields. For all the data presented here the spheromaks had opposite magnetic helicity, i.e., both the poloidal and toroidal fields were opposed at the reconnection layer. Counterhelicity merging of coaxial spheromaks corresponds locally to a nearly two-dimensional reconnection layer [7]. We are able to change the orientation of the poloidal flux in both the east and west spheromak on subsequent shots (while keeping the toroidal orientation in each fixed). A switch from right-left merging to left-right merging corresponds to a $\approx$90° rotation of the local two-dimensional reconnection plane. In this way we can arrange to have our energy analyzer diagnostic either in or out of the reconnection plane. In both Figs. 1 and 2 we depict the east (west) spheromak with left- (right-) handed helicity so that the energy analyzer is in the reconnection plane. A local Cartesian coordinate system is assigned in each figure.

The retarding grid energy analyzer (RGEA) consists of a series of grids to suppress electrons (-10 V) and to discriminate ions according to their energy (0–100 V) in front of a biased Faraday cup for ion collection (-30 V). The analyzer sits outside the flux conservers (about 50 cm away) and looks between them so that it measures only particles escaping from the reconnection layer. Spheromaks communicate across a 2-cm gap via large (12 cm by 9 cm) chevron-shaped slots cut in the back of each flux conserver. Since the spheromaks are formed by external plasma guns, the stray magnetic field and neutral gas levels in the gap are small. The slots force a macroscopic scale of 12 cm (comparable to the spheromak minor radius). The remaining copper in the back walls provides stability against tilting.

In Fig. 3 we present two projections of the magnetic-field vectors (in the x-$y$and x-z planes) at five locations across the layer at two different times. The probe separation is 2 cm. For this shot, the east (west) spheromak had left- (right-) handed helicity so that the energy analyzer is in the reconnection plane (as depicted in Figs. 1 and 2). Note that at $t_1 = 33$ μs [Fig. 3(b))] a reconnection layer has formed with opposed poloidal and toroidal fields (the magnitude of the largest magnetic field vector is about 1100 G). The thickness of the reconnection layer is evidently about 2 cm, consistent with our value of c/ω_{pi}. At $t_2 = 43$ μs [Fig. 3(b)] much of the poloidal flux has been annihilated. We have verified the thickness of the layer with a higher-resolution probe array. In Fig. 4 we show the poloidal field and the inferred

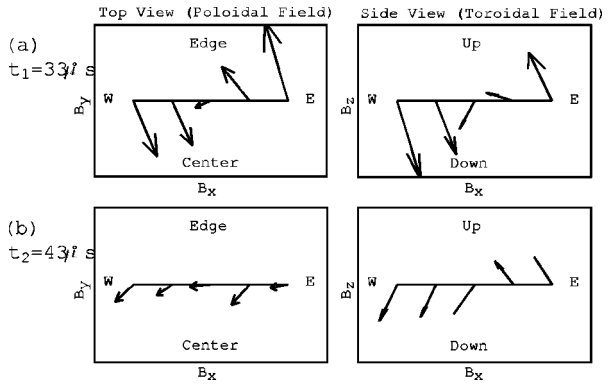

FIG. 3. Reconnection data: (a) t_1 before annihilation; (b) t_2 after annihilation, 10μs later. The two views are projections of the magnetic-field vectors into the horizontal (x-y) and vertical (x-z) planes. Probe separation is 2 cm; $B_{max} \simeq 1100$ G.

$J_z \sim \partial B_y / \partial x$ for a shot similar to that shown in Fig. 3 at t_1. Here, the width of the current layer is $\simeq 2$ cm, consistent with c/ω_{pi}.

Correlated with this flux annihilation event is a delayed burst of plasma flow. In Fig. 5 we present the magnetic energy density around the layer [Fig. 5(a)] and the signal on the RGEA (proportional to energetic ion flux) [Fig. 5(b)] for the same shot as in Fig. 3. The magnetic energy density is defined as $W = (1/N)\Sigma B^2/2\mu_0$, where the sum extends over the $N = 5$ probe locations. We note a peak in the magnetic energy density as the layer is formed followed by a peak in the energetic ion flux. The delay between the annihilation of magnetic flux (drop in magnetic energy) and the appearance of energetic ions 50 cm away is about 5 μs, which gives an ion flow velocity of about v_{Alf} for this event (10^7 cm/s). The later peak is due to a recovery of the spheromak fields and reestablishment of the layer.

We have performed scans of the retarding grid voltage to determine the average energy of the peak ion flux. In Fig. 6 we present escaping ion flux data as a function of energy for a single spheromak [Fig. 6(a)], two merging spheromaks but with the detector out of the reconnection plane [Fig. 6(b)], and two merging spheromaks with the detector in the reconnection plane. We have fit the data to the form $\Gamma = \Gamma_0 \exp(-V/\overline{E})$, where $\overline{E}$ is the average energy. Although the neutral pressure in the gap is low ($P_{base} = 10^{-8}$ torr), some plasma may be present to thermalize the ion distribution. If the density in the gap is $n_e = 10^{14}$ cm^{-3}, then the energetic ion mean free path is 20 cm, which may be sufficient to thermalize the distribution in 50 cm. The ions could

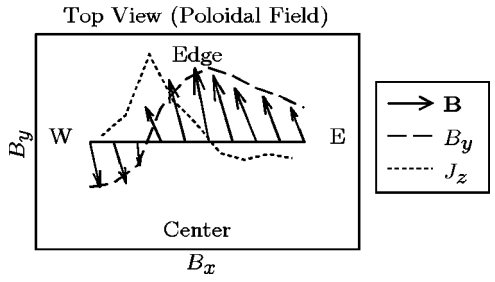

FIG. 4. Detail of reconnection layer in the horizontal (x-y) plane at about t_1. Probe separation is 1 cm; $B_{max} \simeq 930$ G.

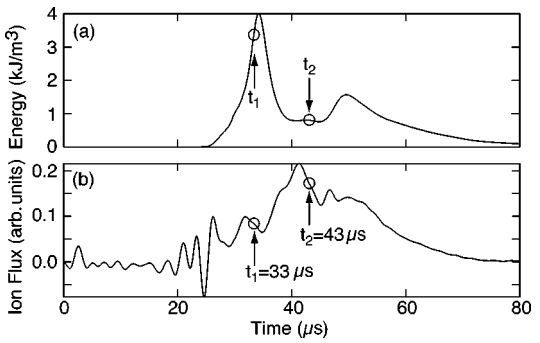

FIG. 5. Time history of the shot in Fig 3: (a) local magnetic energy density; (b) energetic ion flux.

also have been generated with a thermal distribution. In any case, there are clearly more energetic ions in the plane of reconnection. Note that for both the single spheromak and the out-of-plane reconnection case, the average energy is low ($\overline{E} = 30$ and 23 eV, respectively) and consistent with the expected ion temperature (assuming that $T_i \simeq T_e$, as is normally the case in spheromaks). The out-of-plane thermal ion flux is (within errors) simply twice that of a single spheromak ($\Gamma_0 = 0.31$ and 0.14, respectively). The in-plane reconnection flux [Fig. 6(c)] is 25% larger than the out-of-plane flux ($\Gamma_0 = 0.39$) but more importantly the flux is at significantly higher average energy ($\overline{E} = 68$ eV). The velocity of 68 eV protons corresponds to the Alfvén speed at $n_e \approx 10^{14}$ cm^{-3} and $B \approx 500$ G, which is consistent with our probe measurements, so the in-plane flow is due to Alfvénic and not thermal ions.

We do not measure super-Alfvénic ion flux normal to the layer as predicted by Matthaeus *et al.* [18]; however, such flux is expected to be of several orders of magnitude lower intensity than the Alfvénic jets across the layer. We do not have the energy resolution or sensitivity in the current experiment to measure this effect. We also do not have evidence of a super-Alfvénic electron jet or out-of-plane magnetic field at the c/ω_{pe} scale, as predicted by Shay *et al.* [19]. We do not have the spatial resolution to measure such an

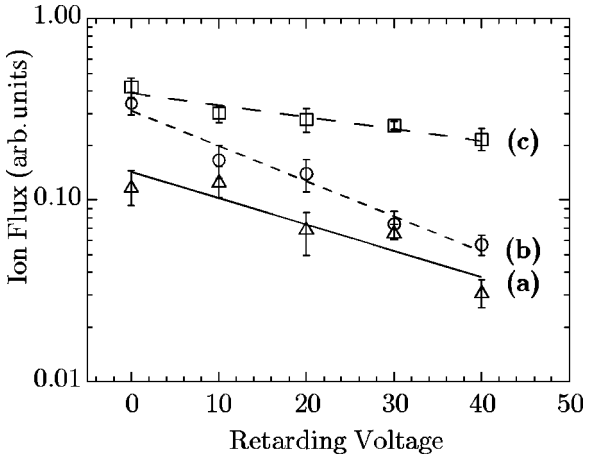

FIG. 6. Retarding energy analyzer scan: (a) single spheromak, thermal ions, and $\overline{E} = 30$ eV; (b) merging spheromaks (out-of-plane), thermal ions, and $\overline{E} = 23$ eV; and (c) merging spheromaks (in-plane), Alfvénic ions, and $\overline{E} = 68$ eV.

effect ($c/\omega_{pe} \approx$ 0.5 mm in our experiment). We should also note that the limited spatial resolution of our linear magnetic probe array does not allow us to observe the dynamics of the entire layer. A three-dimensional magnetic map of the layer is planned.

To summarize, we have experimentally observed correlated magnetic reconnection and energetic ion events at SSX. The most energetic events are jets localized to the plane containing the reconnecting poloidal flux and are consistent with Alfvénic flow. The thickness of the layer is consistent with two fluid collisionless theory and is not consistent with the predictions of resistive MHD.

This work was performed under U.S. DOE Grant No. DE-FG02-97ER54422. P.K.S. was supported by the DESGC. Special thanks are due to S. Palmer for construction of the apparatus.

[1] S. Masuda *et al.*, Nature (London) **371**, 495 (1994).
[2] M. J. Aschwanden *et al.*, Astrophys. J. **464**, 985 (1996).
[3] M. J. Aschwanden *et al.*, Astrophys. J. **447**, 923 (1995).
[4] K. Shibata *et al.*, Astrophys. J. **451**, L83 (1995).
[5] D. E. Innes *et al.*, Nature (London) **386**, 811 (1997).
[6] J. Birn *et al.*, J. Geophys. Res. **86**, 9001 (1981).
[7] M. Yamada *et al.*, Phys. Rev. Lett. **65**, 721 (1990).
[8] M. Yamada *et al.*, Phys. Fluids B **3**, 2379 (1991).
[9] Y. Ono *et al.*, Phys. Fluids B **5**, 3691 (1993).
[10] Y. Ono *et al.*, Phys. Rev. Lett. **76**, 3328 (1996).
[11] M. Yamada *et al.*, Phys. Rev. Lett. **78**, 3117 (1997).
[12] H. Ji *et al.*, Phys. Rev. Lett. **80**, 3256 (1998).
[13] W. Gekelman *et al.*, J. Geophys. Res. **87**, 101 (1982).
[14] C. G. R. Geddes *et al.*, Phys. Plasmas **5**, 1027 (1998).
[15] P. A. Sweet, *Electromagnetic Phenomena in Cosmical Physics*, edited by B. Lehnert (Cambridge University Press, London, 1958).
[16] E. N. Parker, J. Geophys. Res. **62**, 509 (1957).
[17] D. Biskamp *et al.*, Phys. Rev. Lett. **75**, 3850 (1995).
[18] W. H. Matthaeus *et al.*, Phys. Rev. Lett. **53**, 1449 (1984).
[19] M. A. Shay *et al.*, J. Geophys. Res. **103**, 9165 (1998).
[20] H. Ji *et al.*, Rev. Sci. Instrum. **62**, 2326 (1991).